ANALYSIS OF THE PROPERTIES OF RFSSW LAP JOINTS OF ALCLAD 7075-T6 ALUMINUM ALLOY SHEETS UNDER STATIC AND DYNAMIC LOADS

Analiza właściwości połączeń zakładkowych blach ze stopu aluminium 7075-T6 Alclad zgrzewanych metodą RFSSW w warunkach obciążeń statycznych oraz dynamicznych

Andrzej KUBIT ORCID 0000-0002-6179-5359
Koen FAES ORCID 0000-0002-5766-4479
Wojciech JURCZAK ORCID 0000-0002-1608-7249
Magdalena BUCIOR ORCID 0000-0002-1081-5065
Rafał KLUZ ORCID 0000-0001-6745-294X

DOI: 10.15199/160.2020.4.1

A b s t r a c t: This paper presents research regarding refill friction stir spot welding (RFSSW) of EN AW-7075-T6 Alclad aluminium alloy sheets, and the joint behaviour under static and dynamic loads. Single-point lap joint of sheets with different thicknesses, which corresponds to those used in aircraft fuselage structures, i.e. upper sheets with a thickness of 1.6 mm and lower sheets with a thickness of 0.8 mm, were analysed regarding the failure mechanism in static shear testing. It has been shown that a properly made joint is destroyed as a result of tension in the lower plate. The lower plate at the edge of the weld is structurally weakened by the HAZ, but also geometrically due to plastic deformation during the welding process, which has been demonstrated by metallographic investigations as well as by the FEM numerical model. Single-row RFSSW welded joints with different spacing of the welds and a riveted joint were impact tested. It has been shown that welded joints are characterized by a greater stiffness, which is higher when the spacing of the welds is smaller.

K e y w o r d s: RFSSW, aircraft fuselage skin, aluminium alloy, drop-weight impact test, FEM, impact resistance

S t r e s z c z e n i e: Praca przedstawia badania połączenia zakładkowego RFSSW blach ze stopu aluminium EN AW-7075-T6 Alclad pod wpływem obciążeń statycznych oraz dynamicznych. Jednopunktowe połączenie zakładkowe blach o różnej grubości co odpowiada połączeniom stosowanym w konstrukcjach kadłubów lotniczych tj. górna blacha o grubości 1.6 mm oraz dolna blacha o grubości 0.8 mm, poddano analizie mechanizmu zniszczenia w próbie statycznego ścinania. Wykazano, że poprawnie wykonane połączenie ulega zniszczeniu na skutek rozciągania dolnej blachy. Dolna blacha przy krawędzi zgrzeiny jest osłabiona strukturalnie przez strefę wpływu ciepła, ale także geometrycznie poprzez deformację plastyczną powstałą podczas procesu zgrzewania, co wykazano na podstawie badań metalograficznych jak również przy użyciu modelu numerycznego MES. Jednorzędowe połączenia zakładkowe poddano badaniom udarności. Badano połączenia zgrzewane RFSSW o różnym rozstawie zgrzein oraz połączenie nitowane. Wykazano, że połączenia zgrzewane charakteryzują się większą sztywnością, która jest tym większa im mniejszy rozstaw zgrzein.

S ł o w a k l u c z o w e: zgrzewanie RFSSW, pokrycia kadłubów lotniczych, badania dynamiczne z użyciem młota opadowego, MES, odporność na uderzenia

Introduction

A relatively new technology for joining construction materials, especially unweldable metals, is the friction stir welding method. Refill Friction Stir Spot Welding (RFSSW) is a derivative of this process and combines many advantages, so it may soon become an alternative to traditional joining methods.

One of the areas of industry where the RFSSW welding method can be widely used is the aviation industry. In this industry, there is a great demand for technologies ensuring structural joints with high strength, which could be used for the construction of thin-walled stiffened structures.

Despite the undisputed advantages of the RFSSW technology over riveting, this technology, being relatively new, is not yet fully understood. Controlling the parameters of the welding process means that there are many combinations of parameters which translate into different conditions and, consequently, different quality levels of the joint in terms of strength and structure. As part of the research carried out by the authors of this work, parameters of the welding process were selected to ensure a high load-bearing capacity and the required quality of the joint structure in the variant under consideration, as presented in the works [10, 11].

Loads of static forces and cyclically repeating variable loads causing fatigue are the basic, but incomplete

spectrum of operational loads of stiffened thin-walled structures, used, among others, in aircraft construction. An important issue that should be considered in the tests of this type of structure is damage due to random events causing dynamic loads.

Aviation structures can be exposed to many dynamic impact events. Basically, in civil aviation, such events can be divided into two groups. The first is the collision of an aircraft with a foreign object during the flight [17]. These are mainly the impacts of ice blocks during hail [8, 9], as well as collisions with birds [4, 19]. These types of damage to aircraft structures are generally associated with a high impact velocity and a relatively low mass of the object.

However, most damage of aircraft structures as a result of random foreign object strikes in civil aircraft occurs primarily in ground handling [6]. Then, accidental impacts occur during loading or unloading, and this is the most common form of damage to the structural elements of an aircraft [6]. Dynamic impacts of aircraft skins during maintenance are also common. Finally, there are cases of collisions with objects, e.g. during taxiing [3].

Ground damage cases caused by dynamic impacts are characterized by a relatively low impact speed, as well as a significant mass of the objects defined as foreign bodies. The authors of the studies [5, 14, 16] defined the speed range for collisions classified as low speed in the range of 1-10 m/s. In practice, however, the impact speed are usually around 2 m/s [4]. Therefore, when carrying out experimental research or modelling phenomena occurring in the considered events, they are considered as quasi-static phenomena [3, 4]. With low-speed impacts, the contact between the object and the structure is so long that the entire structure carries a dynamic load, similar to a static load [1, 15].

Charpy and Izod tests as well as drop weight tests are commonly used for impact testing with low impact velocities [16]. In the case of impact strength tests of aircraft structures, the last of the mentioned methods most precisely reflects the conditions of real random events related to dynamic loading of the structure [2, 13].

This paper presents the results of tests of RFSSW joints subjected to static shear tests. The failure mechanism was analysed based on metallographic investigations. Modelling of the welding process using the FEM method was also performed in order to theoretically determine the mechanical phenomena occurring during joining the sheets. In the next step, comparative tests of single-row RFSSW lap joints and riveted joints subjected to the impact bending test were carried out. Since the considered joint is being analysed in terms of the possibility of using it as an alternative form of joining of thin-walled structures, where rivets are commonly used, therefore, comparative tests were carried out. The comparative tests were carried out for single-row lap joints typically found in thin-walled aircraft structures. The drop weight impact test was carried out. The justification for conducting such tests is the exposure of thin-walled structures to various types of random events that may be associated with a dynamic impact on the structure.

Materials and method

The tests were carried out for overlap joints of sheets with different thicknesses, corresponding to the stringer and the skin, based on the example of a thin-walled aircraft structure. It was assumed that both elements would be made of EN AW-7075-T6 aluminium alloy. This alloy is characterized by a high static and fatigue strength [11]. It is difficult to deform the material plastically as the yield point is close to the tensile strength [11]. Moreover, the material is difficult to weld and has a relatively low corrosion resistance [11]. The basic feature, which is a high strength while maintaining a low weight, makes this material widely used in the construction of aircraft structures. Due to the relatively high susceptibility to intercrystalline corrosion, the sheets used in the construction of thin-walled aircraft structures are usually clad, i.e. covered with a thin (about 5% of the thickness of the parent material) layer of technical aluminium, i.e. almost pure aluminium, in the hot rolling process. Fig. 1 shows a microscopic view of a 1.6 mm thick sheet with the visible clad layer.

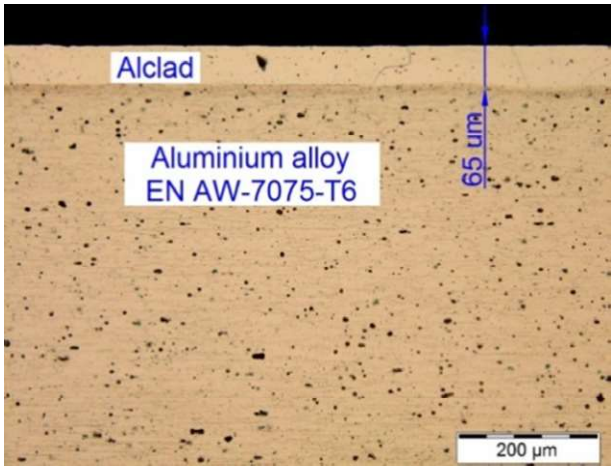

Fig. 1. Microscopic view of the sheet used in the tests with a visible layer of the alclad

For the sheets used, the mechanical properties were determined in static tensile tests according to EN ISO 6892-1: 2016 [7]. The tests were made for three different directions in relation to the rolling direction of the sheet, i.e. 0 °, 45 ° and 90 °. Five repetitions were performed for each of the directions. Table 1 summarizes the values of the basic parameters determining the mechanical properties of the material used.

Single-point lap joints with the dimensions shown in Fig. 2 were subjected to static tests. The welded joints were made with the use of a special machine for RFSSW spot welding, i.e. RPS100 VA11 by Harms & Wende GmbH & Co KG (Hamburg, Germany). The samples

Table 1. Basic mechanical properties of 7075-T6 aluminium alloy sheets

Parameter	Young's modulus E MPa	Yield stress Rp0.2, MPa	Ultimate tensile strength Rm, MPa
Value	70316	463	530

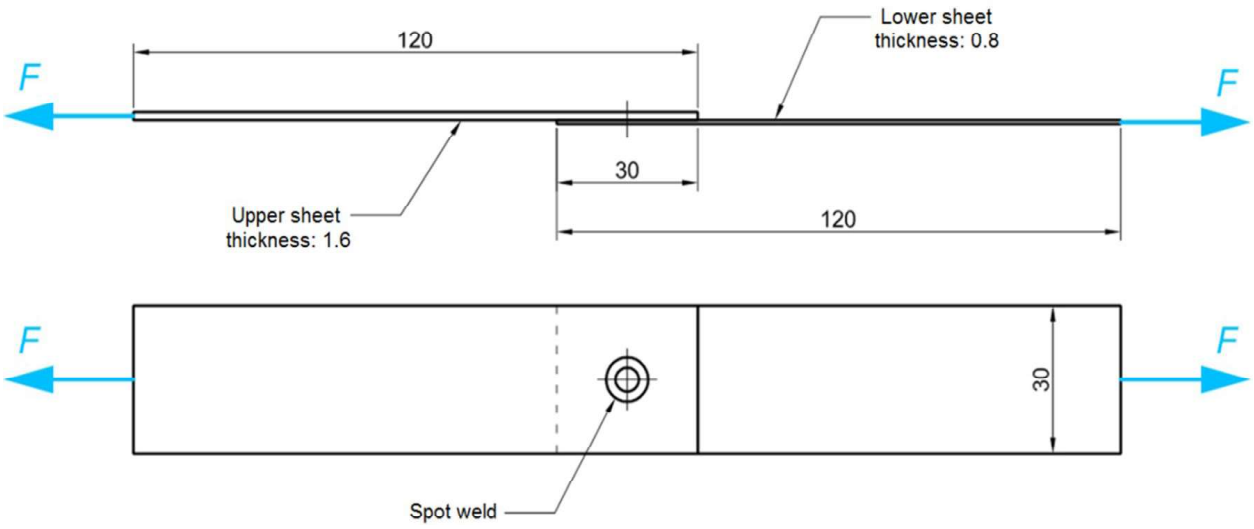

Fig. 2. Shape and dimensions (in mm) of the welding specimens

used in the tests were made using the following welding parameters: tool rotational speed n = 2400 rpm, sleeve plunge depth g = 1.55 mm and welding time t = 3.5 s.

The tests of static strength were carried out at room temperature on a Zwick / Roell Z100 testing machine, the jaw feed rate was 5 mm/min.

Microstructure and fracture morphologies of selected specimens were analysed using a Phenom ProX (Phenom-World B.V., Eindhoven, Netherlands) variable pressure scanning electron microscope (SEM).

The numerical simulation model of the RFSSW process has been conducted using the Simufact Forming software (Simufact Engineering Gmbh, Hamburg, Germany). Due to the symmetrical nature of the process, a 2D axisymmetric simulation was performed.

In FE-based simulations of the welding process, a number of simplifications of the numerical model have been adopted in relation to the real conditions. Individual elements of the tool, i.e. pin, sleeve and clamping ring in the FE model were adopted as cylindrical bodies with smooth surfaces. So, characteristic grooves made on the outer surfaces of the pin and sleeve were omitted. Due to the relatively small plunge depths of pin and sleeve, these grooves do not significantly affect the welding process conditions in the case of joining thin sheets. The sleeve, pin and clamping ring were all considered as rigid bodies. It is well known that the Alclad layers have a significant effect on the heat distribution during the welding process due to the significantly higher thermal conductivity of the Alclad material in relation to the material of base plate. Therefore, the model consists in an intermediate layer between sheets to reflect the properties of the Alclad. The thickness of the Alclad layer in the numerical model was equal sum of the Alclad layers on both upper and lower sheets.

The sheets and Alclad were modelled with 2D elements, destined for analysis of 2D axisymmetric problems, called Quad (10) in Simufact Forming terminology [18]. Rigid tools were modelled with quad elements called Quad (40) [18]. The initial mesh (Fig. 3) has been generated using Advanced Front Quad mesher. During

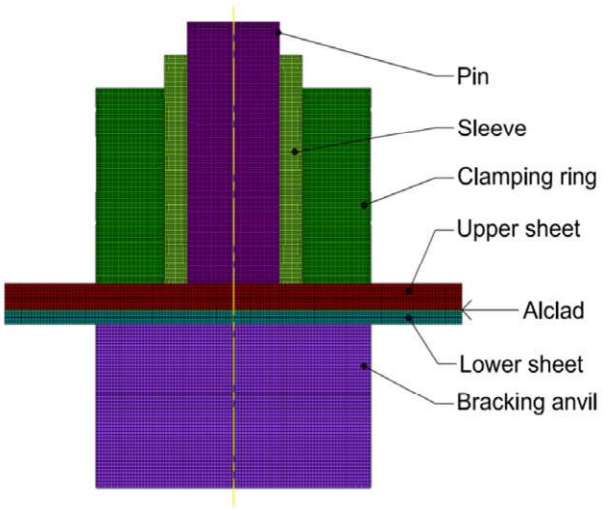

Fig. 3. Finite element mesh of 2D model

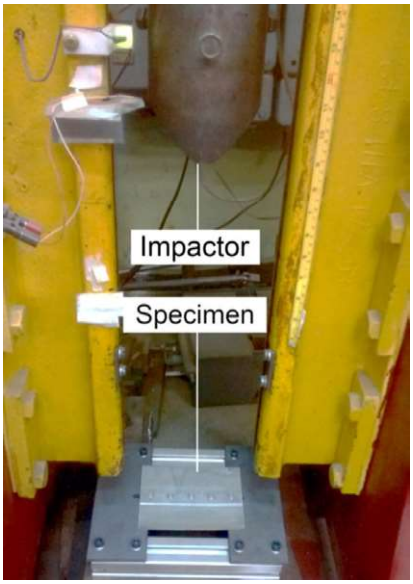

Fig. 4. Drop weight test stand

the simulation of the RFSSW process, the initial mesh gets distorted due to the large displacement and does not fit the required mesh quality anymore. Excessive mesh distortion of the FE-based model leads to divergence problems. To avoid too much distortion of the mesh elements, an automatic remeshing that automatically regenerates the mesh was used and the simulation is continued using the new mesh. The sheets and Alclad models were composed of 3474 elements Rigid bodies consists of 4549 elements.

Impact tests were carried out using a drop weight testing machine. The complete test stand with the test sample is shown in Fig. 4. The element causing the dynamic load by gravity is composed of a drop weight with a mass of 27 kg and an impactor with a mass of 8.81 kg, which gives a total mass of 35.81 kg.

Tests of single-row lap joints were carried out for RFSSW welded joints with different spacing of welds, as well as for riveted joints. The riveted specimens were made with anodized, roll-formed aviation rivets with a mushroom head 3 mm in diameter, made of PA24 aluminium alloy.

Fig. 5 shows the geometry and dimensions as well as the method of supporting the samples of single row joints used in dynamic tests.

In the dynamic load test, the measurements of geometric quantities characterizing the degree of sample deformation were made. The presented configuration of the load is a classic three-point bending, therefore the values of the deflection of the sample were measured. The plastic deflection was determined after the test, while the elastic deflection had to be recorded at the moment the hammer hit the sample. Thus, the registration of the elastic deflection was made by placing plastic masses directly under the sample, which fixed the value of this deflection.

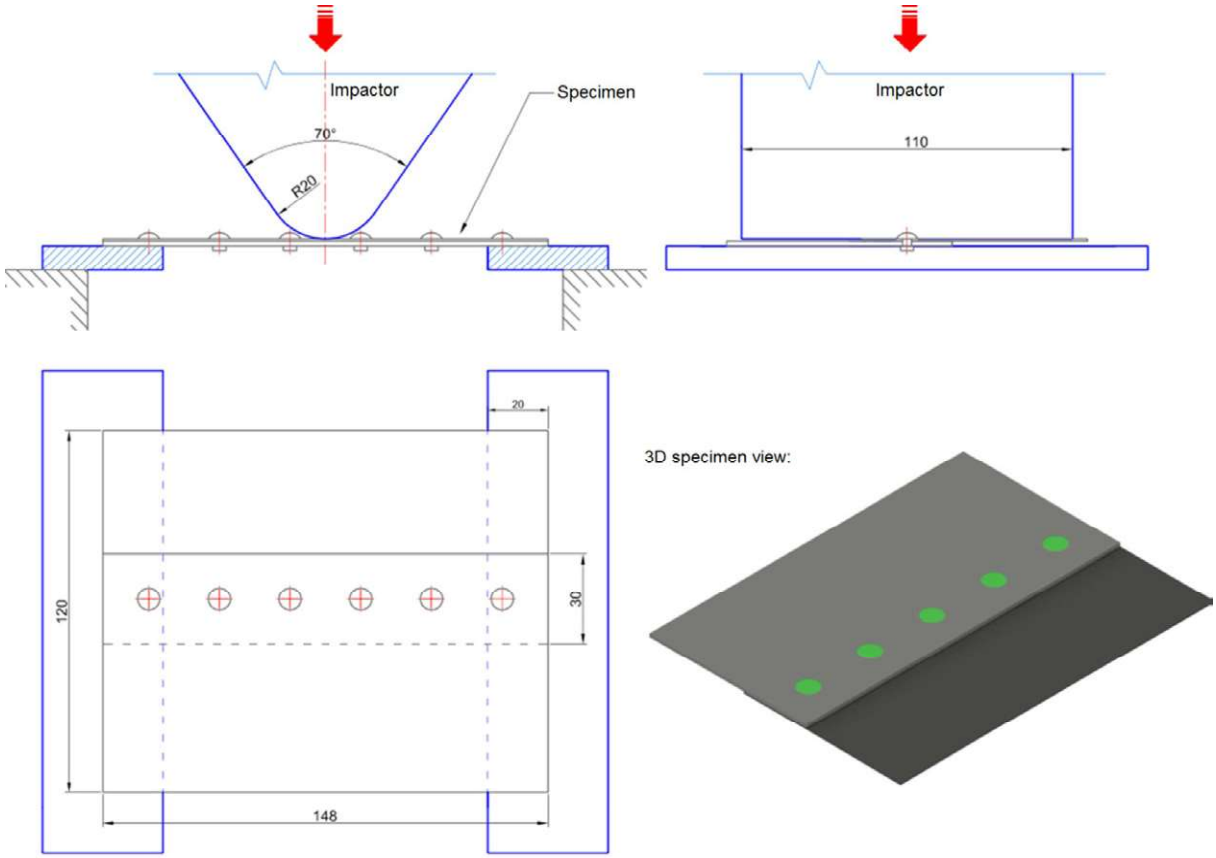

Fig. 5. Dimensions and configuration of the support and loading of the specimen during the impact test

A rivet spacing of 23.5 mm was used, as this value is used in typical thin-walled aircraft structures. In the case of welded joints, two different spacings were used. In the first case, the principle of spacing between the edges of the joints was followed, while maintaining the same dimensions between the edges for welded joints as in the case of riveted joints, which are schematically shown in Fig. 6. Thus, a spacing of 29.5 mm was used. Due to the larger surface area of the welded joint compared to the rivet, the welded samples with a spacing of 50% greater, i.e. 44.25 mm, were additionally tested.

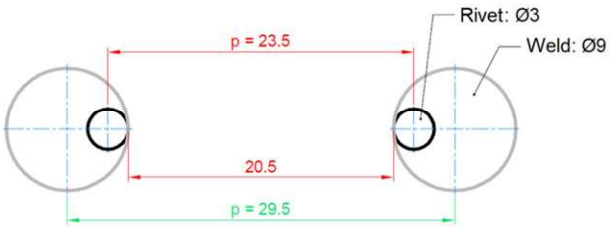

Fig. 6. The diagram illustrating the selection of the basic spacing of welds based on the spacing of rivets

Results

Fig. 7 shows a representative curve obtained in a static shear test for the joined samples considered. It was shown that in case of the welding process parameters used, the failure of the joint was achieved by tension of the lower sheet, while the crack was initiated at the perimeter of the weld in the heat-affected zone (HAZ) (Fig. 8).

The mean value of the load capacity for the five repetitions carried out is 5.78 kN (SD: 47.20 N). The demonstrated method of sample destruction proves the high strength of the joint itself, which was not sheared. The crack in the sheet in tension is not the result of the load reaching the Rm value of the material used. Directly at the weld, due to thermo-mechanical phenomena, the sheet was locally weakened, assuming lower strength parameters than the parent material in the T6 state.

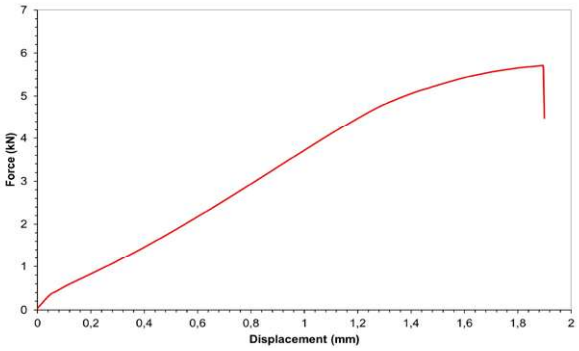

Fig. 7. Representative curve Force-Displacement obtained in a static shear test for single-lap joints

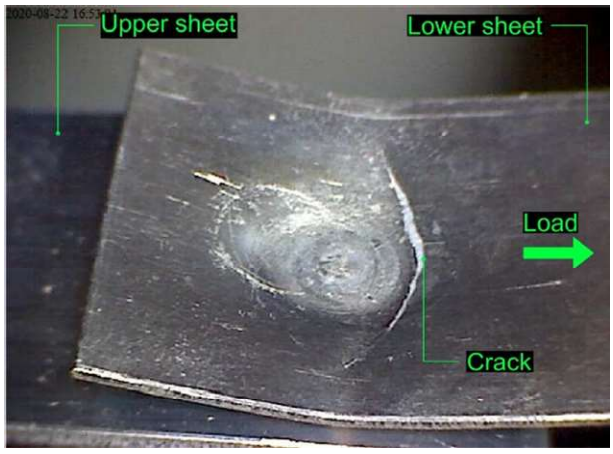

Fig. 8. View of the lower sheet with a visible crack due to tensile stress at the perimeter of the weld

It was observed that the lower sheet was deflected before it cracked due to the bending moment. The failure mechanism of the joint in question is strictly dependent on the configuration of the sheets to be joined. As the sheets have different thicknesses, hence a significant difference in their stiffness leads to an asymmetric state of stresses when loading the lap with an axial force. Fig. 9 shows the stresses that arise in the joint during its loading with uniaxial force.

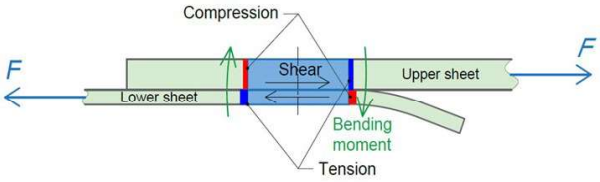

Fig. 9. Stresses in the lap joint caused by uniaxial tensile force

When the critical stress value is exceeded, the bottom plate cracks at the perimeter of the weld. Based on the metallographic analysis, it was shown that in the joint forming process, plastic deformation of the lower sheet occurs caused by the material pressed through the sleeve at the end of the process (Fig. 10). This phenomenon was confirmed on the basis of the FEM numerical model. Figs. 11a, b show the final stage of the simulation of the joint creation, indicating the phenomena taking place in the material on the basis of the accumulated plastic strain (Fig. 11a) and also the displacement vector (Fig. 11b). This deformation along the periphery of the weld leads to a reduction in the cross-sectional area of the lower plate, which in turn results in cracking at that location. Additionally, in the place where the cracking of the sheet was found, the material was weakened by the influence of the heat-affected zone. Regarding the fracture, a typical separation ductile fracture was observed, which is due both to the direction of the fracture (fracture at an angle of about 45°) and the nature of the fracture surface shown in the SEM image - Fig. 12.

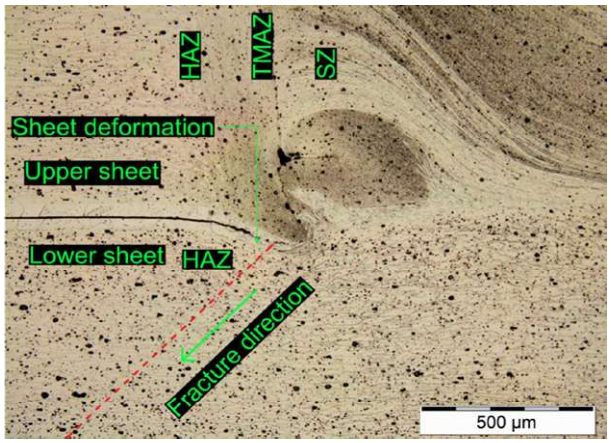

Fig. 10. Macroscopic image of the weld corner with visible deformation of the lower sheet and with the direction of cracking marked

In the tests, the assumed impact energy was 26.3 J, which corresponds to the hammer height of 75 mm. As a result, an impact velocity of 1.33 m/s was obtained. After the impact, the plastic and elastic deflections at the moment of impact were measured. Table 2 summarizes the average values of the measured values for individual variants.

Each of the joint points was also verified, assessing whether they were damaged or not. Fig. 13 shows samples for each variant. In the case of samples welded in both considered spacings, the welds were coherent (Figs. 13b, c). In the case of the riveted joint (Fig. 13a), the two extreme rivets were sheared. The microscopic images (Fig. 14) clearly show that there was a relative shift of the sheets due to the bending of the overlap, and thus the rivets were sheared in the plane of the sheet connection.

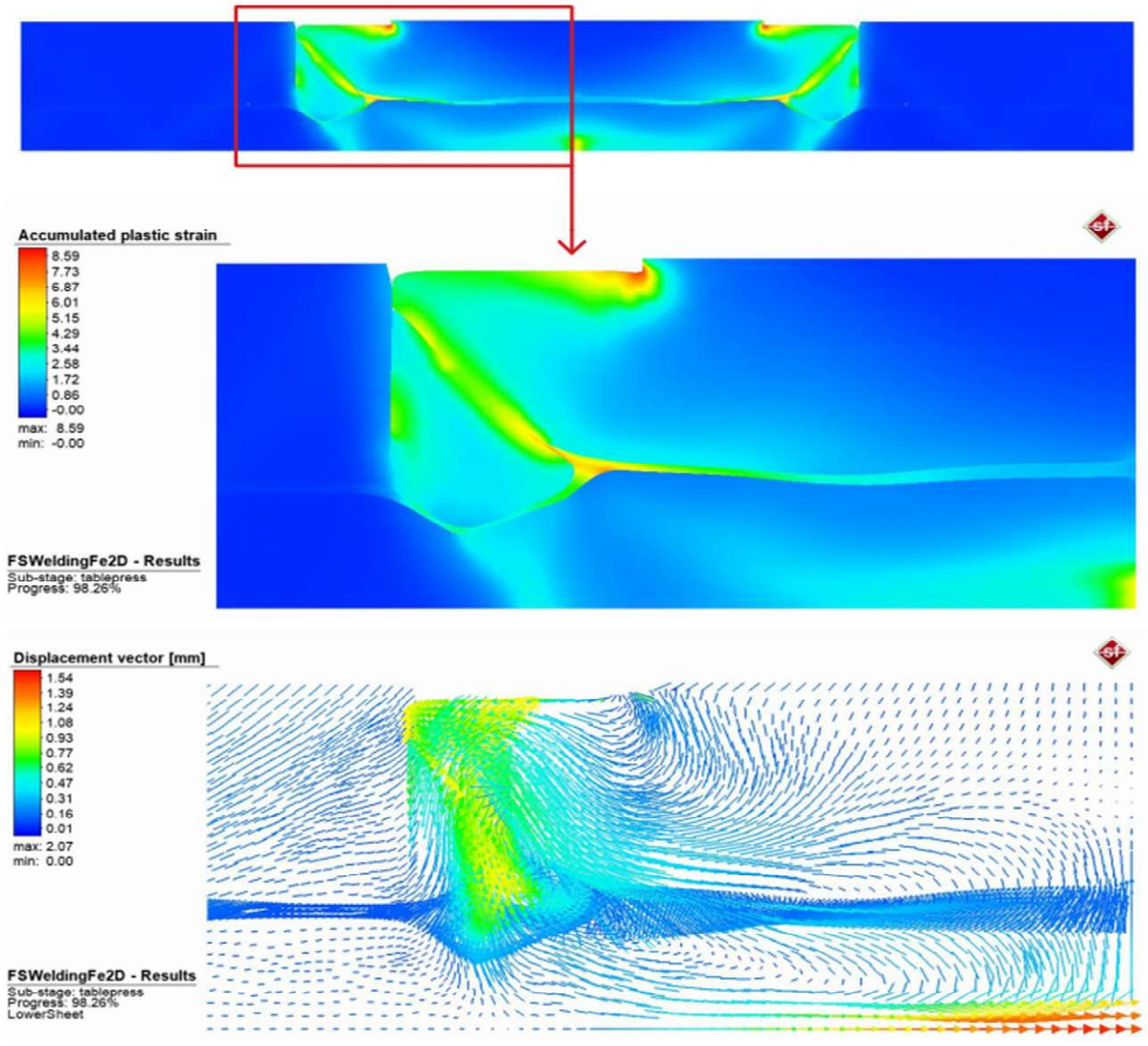

Fig. 11. View of the deformation in the weld zone at 98.26% of the RFSSW cycle: a) accumulated plastic strain, b) displacement vector (mm)

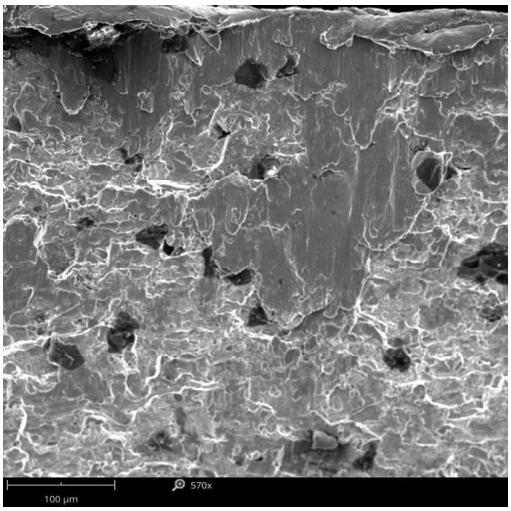

Fig.12. SEM micrograph showing the fracture surface morphology of lower sheet

Based on the test results, it has been shown that the RFSSW joint is more rigid than the rivet joint. This is influenced by various factors. The lower stiffness of the riveted joint is due to the holes in the sheets, in addition, the total area of the joint is greater in the case of welded variants (rivet diameter is 3 mm, weld diameter - 9 mm). It should also be noted that in the presented tests, the extreme rivets sheared, which also had an impact on the reduction of joint stiffness. It has also been shown that the stiffness of the welded joint is higher for a smaller spacing of the welds.

Fig. 15 shows SEM images of the chamfer surface of rivet 1 (Fig. 15a). In a small fracture area at the edge of the rivet, a brittle fracture can be observed, as shown by the SEM images shown in Figs. 15b, c. The area where brittle fracture occurs is at the edge at which the fracture initiated under dynamic loading. However, the dominant form of failure in the dynamic bending test was plastic

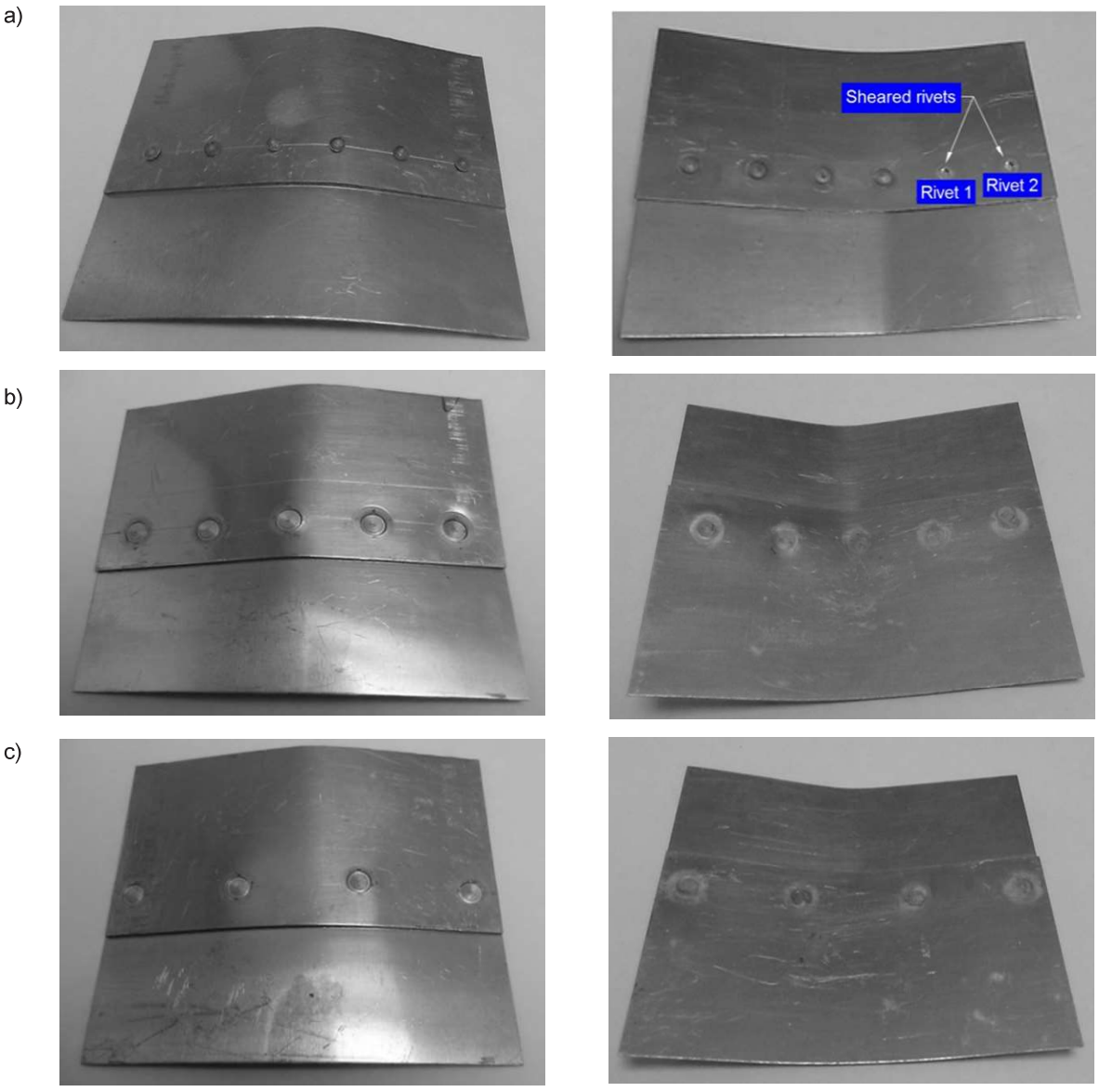

Fig.13. Lap joints of flat sheets after impact tests: a) riveted joint with a spacing of 23.5 mm, b) joint made with the RFSSW technology with a weld spacing of 29.5 mm, c) joint made with the RFSSW technology with a spacing of 44.25 mm

Table 2. Results of measurements of deflection under the influence of dynamic impact of lap samples

Lp.	Specimen variant	Impact energy J	Impact velocity m/s	Plastic deflection [mm]	Plastic+elastic deflection [mm]
1	Riveted joint with a spacing of 23.5 mm	26.3	1.33	12.9	13.6
2	Welded joint with a spacing of 29.5 mm	26.3	1.33	9.4	10.9
3	Riveted joint with a spacing of 44.25 mm	26.3	1.33	9.7	11.3

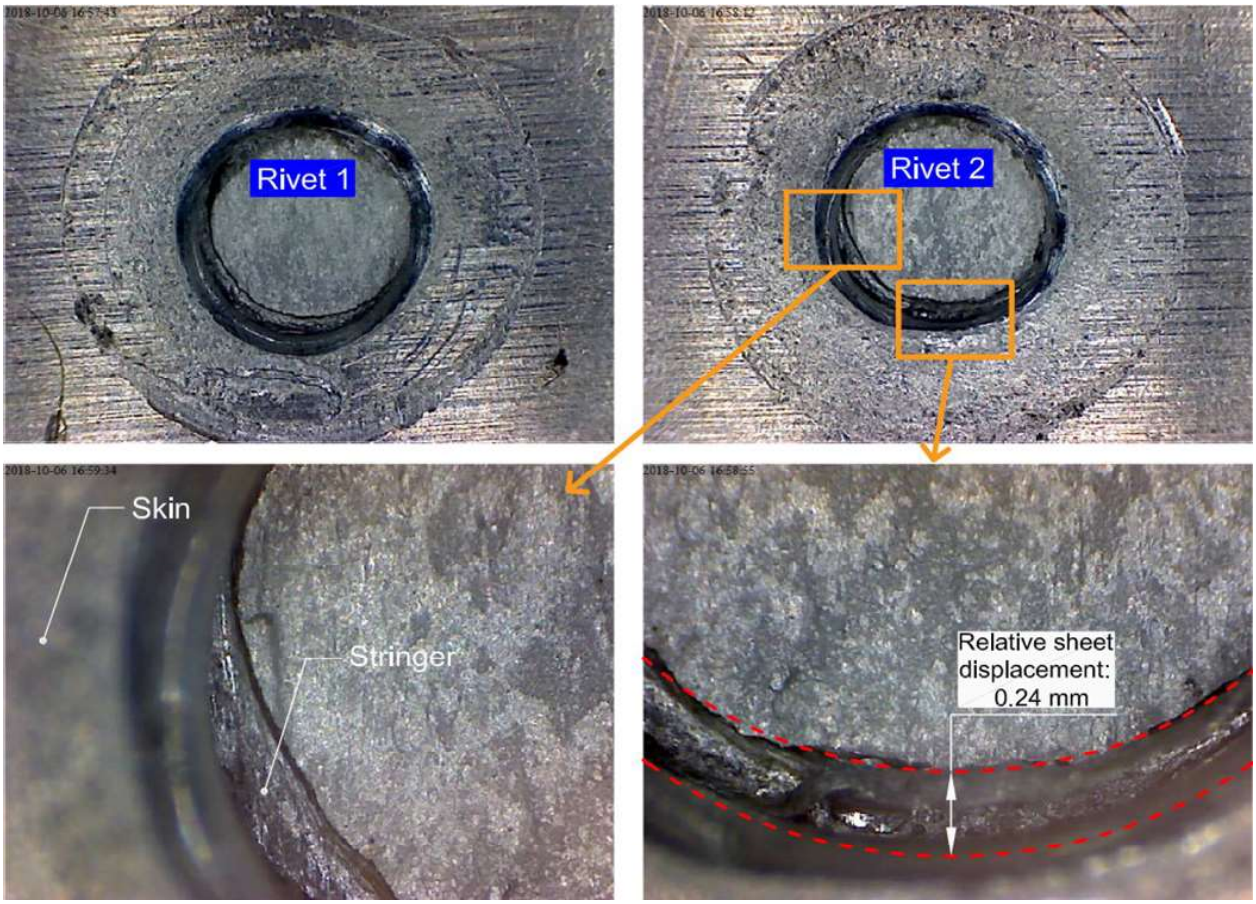

Fig. 14. Macroscopic images of the sheared surfaces of the rivets showing the relative displacement of the joined sheets

cracking that occurs on the remainder of the surface. In the central region of the fracture of the rivet, dimples of different sizes were shown, which are typical for ductile fracture (Figs. 15d, e). From the views of the fracture, typical ductile cracking can be observed, characterized by the formation of pits, i.e. pits and craters. It is the effect of material flow, the phenomenon of cracking took place here by nucleation and growth of voids. In the area marked by points f and g in Fig. 15a, a plastic breakthrough is primarily shown (Figs. 15f, g).

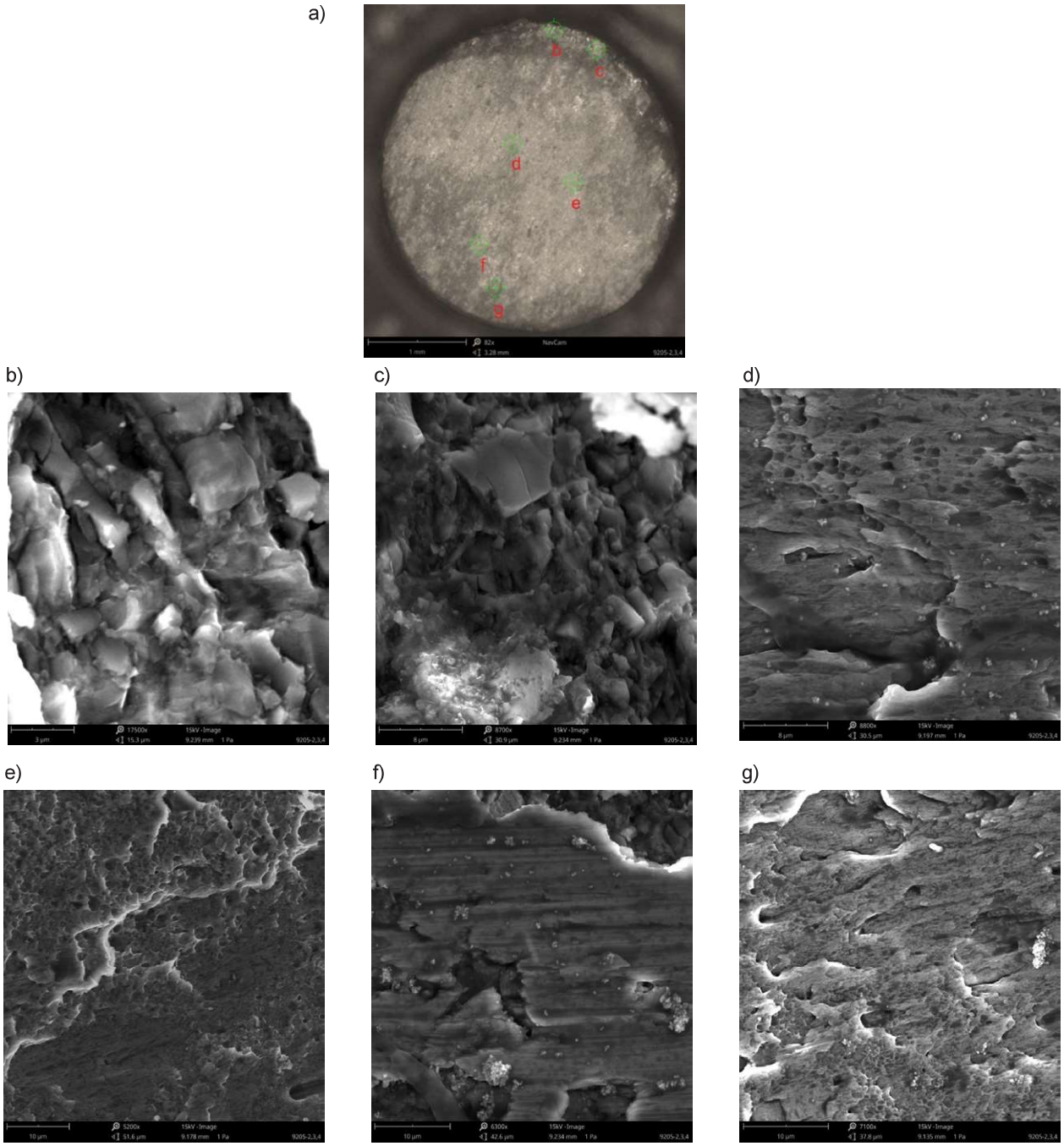

Fig. 15. Fracture surface of sheared rivet: a) macrograph of whole surface; b) - g) SEM micrographs showing the fracture surface morphology of characteristic areas

Conclusions

One of the objectives of the research presented in the paper was to experimentally determine the mechanism of failure of lap joints made by the RFSSW method in the static shear test. It has been shown that a correctly created joint of sheets made of the EN AW-7075-T6 Alclad alloy with thicknesses corresponding to the stringer (thickness 1.6 mm) and the skin sheet (0.8 mm) is fractured in the static shear test as a result of tensile stress of the thinner sheet. This is due to the weakening of the material in the HAZ, but also the deformation occurring during welding, which leads to a reduction in the cross-section of the sheet, which was demonstrated on the basis of the joint macrostructure and the FEM numerical model. Before failure, the lower sheet undergoes plastic deflection due to the bending moment resulting from the joint geometry used.

References

[1] Bryan H. 1999. Engineering Composite Materials. London: The Institute of Materials.

[2] Cantwell W.J., Morton J. 1991. "The impact resistance of composite materials – a review". Composites 22(5): 347-362.
[3] Chen Z.M., Kim H., DeFrancisci G.K. Experimental and Modeling Investigation of Blunt Impact to Stringer Reinforced Composite Panels. COVER SHEET.
[4] DeFrancisci G.K., Chen Z.M., Kim H.: Blunt impact damage formation in frame and Stringer stiffened composite panels. 18th International Conference on Composite Materials.
[5] Elber W., Shivakumar K.N., Illg W. 1985. "Prediction of low velocity impact damage in thin circular laminates". American Institute of Aeronautics and Astronautics Journal 23(3): 442-449.
[6] International Air Transportation Association. 2005. Ground Damage Prevention Programme Targets 10% Cost Reduction. Industry Times, Article 4.
[7] ISO 6892-1:2016. 2016. Metallic materials — Tensile testing — Part 1: Method of test at room temperature. Switzerland, Geneva: International Organization for Standardization.
[8] Kim H., Kedward K.T. 2000. "Modeling Hail Ice Impacts and Predicting Impact Damage Initiation in Composite Structures". AIAA Journal 38(7): 1278-1288.
[9] Kim H., Kedward K.T., Welch D.A. 2003. "Experimental Investigation of High Velocity Ice Impacts on Woven Carbon/Epoxy Composite Panels". Composites Part A 34(1): 25-41.
[10] Kubit A., Bucior M., Wydrzyński D., Trzepieciński T., Pytel M. 2018. "Failure mechanisms of refill friction stir spot welded 7075 – T6 aluminium alloy single – lap joints". International Journal of Advanced Manufacturing Technology 94(9-12): 4479-4491.
[11] Kubit A., Kluz R., Trzepieciński T., Wydrzyński D., Bochnowski W. 2018. "Analysis of the mechanical properties and of micrographs of refill friction stir spot welded 7075 – T6 aluminium sheets". Archives of Civil and Mechanical Engineering 18(1): 235-244.
[12] Kubit A., Kluz R., Trzepieciński T. 2020. "A fully coupled thermo-mechanical numerical modelling of the refill friction stir spot welding process in Alclad 7075-T6 aluminium alloy sheets". Archives of Civil and Mechanical Engineering 20(117): 1-14.
[13] Mendez P.F., Eagar T.W. 2001. "Welding process for aeronautics". Advanced Materials and Processes 159: 39-43.
[14] Niewerth D., Stefaniak D., Hühne C. 2014. The response of hybrid composite structures to low-velocity impact. 16th International Conference on Experimental Mechanics.
[15] Richardson M.O.W., Wisheart M.J. 1996. "Review of low-velocity impact properties of composite materials". Composites Part A: Applied Science and Manufacturing 27(12): 1123-1131.
[16] Safri S.N.A., Sultan M.T.H., Yidris N., Mustapha F. 2014. "Low Velocity and High Velocity Impact Test on Composite Materials – A review". The International Journal of Engineering and Science 3(9): 50-60.
[17] Schoeppner G., Abrate S. 2000. "Delamination Threshold Loads for Low Velocity Impact on Composite Laminates". Composites: Part A 31(9): 903-915.
[18] Simufact Forming - Theory manual. 2016. Champaign: Computational Applications and System Integration Inc.
[19] Zbrowski A. 2012. „Bezpieczeństwo samolotów w aspekcie zagrożenia kolizją z ptakami". Problemy Eksploatacji 2: 215-227.

dr inż. Andrzej Kubit
Department of Manufacturing and Production Engineering
Rzeszow University of Technology
Al. Powstańców Warszawy 12, 35-959 Rzeszow, Poland
e-mail: akubit@prz.edu.pl

dr. ir. Koen Faes, EWE
Welding Institute
Technologiepark-Zwijnaarde 935, 9052 Gent, Belgium

dr hab. inż. Wojciech Jurczak
Polish Naval Academy
Faculty of Mechanical and Electrical Engineering
ul. Śmidowicza 69, 81-127 Gdynia, Poland

dr inż. Magdalena Bucior
Department of Manufacturing and Production Engineering
Rzeszow University of Technology
Al. Powstańców Warszawy 12, 35-959 Rzeszow, Poland

dr inż. Rafał Kluz
Department of Manufacturing and Production Engineering
Rzeszow University of Technology
Al. Powstańców Warszawy 12, 35-959 Rzeszow, Poland